Modeling of triboelectric separation of plastic particles in electric field

František Mach, Pavel Kůs, Pavel Karban
University of West Bohemia
306 14 Plzen, Univerzitni 26, e-mail: fmach@kte.zcu.cz, pavel.kus@gmail.com, karban@kte.zcu.cz

Ivo Dolezel
Czech Technical University
166 27 Praha 6, Technicka 2, e-mail: dolezel@fel.cvut.cz

A device for electrostatic separation of triboelectrically charged plastic particles is modelled and optimized. Electric field in the system is solved numerically by a fully adaptive higher-order finite element method. The movement of particles in the device is determined by means of an adaptive Runge-Kutta-Fehlberg method. The shape optimization of the electrodes is carried out using a technique based on higher-order conjugate gradients. The methodology is illustrated by a typical example.

1. Introduction

Nowadays, an intensive research aimed at the possibilities of recycling plastic materials is conducted worldwide, because in a lot of applications the recycled materials may well replace the new ones. The necessary prerequisite of this reprocessing is a high-quality separation of particular kinds of plastics preliminarily grinded into small sphere-like particles. One of the advanced techniques of separation of these particles is based on the triboelectric effect. It is known, that when electrically non-conducting particles of two different levels come into contact with electric charge, after charging one of them becomes more positive (or negative) with respect to another one. And their trajectories in electric field (affected by the charge that they carry) may be then quite different.

More accurately, the trajectories of the charged particles moving in electric field are influenced by the Coulomb force exerted on it by this field, mutual force effects among the particles, gravity and drag aerodynamic forces. And these trajectories predetermine their impact points, in other words, the places where they fall down. It is clear from Fig. 1 showing a typical separator of this kind.

The separator consists of two electrodes, one of them being grounded. The voltage of the other electrode is used to be on the order of tens kV. The electrodes may be covered by Teflon or another insulating material that prevents recharging of the particles in case of the direct impact with them. The mixture of charged

particles is delivered by the feeder. At the bottom of the device there are several recycle bins used for accumulating of particular levels of plastics. One of the principal demands is to tune the shape of the electrodes and widths of the bins so that the particles of different levels should fall down exactly to the corresponding bin.

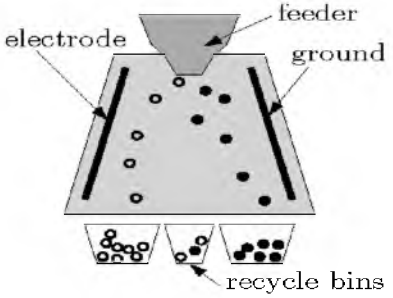

Fig. 1. Basic arrangement of the considered separator

The described kind of triboelectric separation was analyzed by a number of researchers. For example, papers [1–8] are prevailingly aimed at a detailed description of the technology and its practical applications. On the other hand, modeling of the particle trajectories in electric field traps and similar devices (with the aim to appropriately design their arrangement) based on classical finite difference and finite element algorithms can be found in [9–10]. But accuracy of the results was not too high because the distribution of nonuniform electric field and motion of the particles were calculated separately and the computations were based on low-order mapping methods. The problem of the shape optimization of both electrodes and bins was solved rather by a comparison of several different arrangements, without applying direct optimization techniques.

An attempt to fill in the above gaps is the subject of this paper. The distribution of electric field between the electrodes is determined using a fully adaptive higher-order finite element method, i.e., with much higher accuracy than that provided by the mentioned low-order method. The movement of the particles affected by electric field, gravity and drag aerodynamic resistance is modelled by an adaptive Runge-Kutta-Fehlberg method with a time-varying time step. The shape optimization of the electrodes is carried out using a technique based on higher-order conjugate gradients.

2. Continuous mathematical model of the problem

Consider the arrangement in Fig. 1. The particles of plastics of charge Q and initial velocity $\boldsymbol{v}_0$ enter the space between two electrodes. During their movement in the separator they are deflected according to their charge and fall down into the recycle bins (as these charges are low, it is possible to neglect the Coulomb forces

acting among the particles, so that their movement is affected mainly by the external electric field). The task is to find their trajectories and evaluate the influence of the above quantities.

Electric field in the domain of the separator is described by the equation [11] for the electric potential φ

$$\operatorname{div}\left(\varepsilon \operatorname{grad}\varphi\right) = 0\,, \tag{1}$$

where symbol ε stands for the dielectric permittivity. The boundary conditions are given by the known values of the electric potential on the electrodes and the Neumann condition along the artificial boundary placed at a sufficiently distance from the device.

The movement of the particle is governed by the equations for velocity $\boldsymbol{v}$ and trajectory $\boldsymbol{s}$ in the forms

$$m\frac{\mathrm{d}\boldsymbol{v}}{\mathrm{d}t} = \boldsymbol{F}_\mathrm{e} + \boldsymbol{F}_\mathrm{a} + \boldsymbol{F}_\mathrm{g}\,, \quad \boldsymbol{v} = \frac{\mathrm{d}\boldsymbol{s}}{\mathrm{d}t}\,, \tag{2}$$

where $\boldsymbol{F}_\mathrm{e}$ denotes the Coulomb force acting on the particle given by the relation

$$\boldsymbol{F}_\mathrm{e} = Q\boldsymbol{E} = -Q\operatorname{grad}\varphi\,, \tag{3}$$

$\boldsymbol{E}$ denoting the local value of the electric field strength. Symbol $\boldsymbol{F}_\mathrm{a}$ represents the aerodynamic resistance that is given by formula

$$\boldsymbol{F}_\mathrm{a} = -\boldsymbol{v}\frac{1}{2}\rho c S v\,, \tag{4}$$

where c is the friction coefficient (depending on geometry of the particle), ρ denotes the density of ambient air, S is the characteristic surface of the particle and v stands for the module of its velocity. Finally,

$$\boldsymbol{F}_\mathrm{g} = m\boldsymbol{g}\,, \tag{5}$$

where m denotes the mass of the particle and $\boldsymbol{g}$ is the gravitational acceleration.

The corresponding initial conditions read

$$\boldsymbol{v}(0) = \boldsymbol{v}_0\,, \quad \boldsymbol{s}(0) = \boldsymbol{s}_0\,, \tag{6}$$

where $\boldsymbol{s}_0$ is the entry position of the particle in the separator. Equation (2) is strongly nonlinear due to the first and second terms on the right-hand side.

3. Numerical solution

The continuous mathematical model consisting of equations (1) and (2) is solved numerically. We used our own codes Agros2D [12] and Hermes2D [13]. While Hermes2D is a library of highly advanced numerical algorithms for monolithic and fully adaptive solution of systems of generally nonlinear and nonstationary partial differential equations (PDEs) based on the finite element

method of higher order of accuracy, Agros2D is a modular-type powerful user's interface serving for pre-processing and post-processing of the problems solved that also allows writing scripts for numerical solutions of ordinary differential equations. Both codes written in C++ are used for monolithic solving complex coupled problems rooting in various domains of physics. They are freely distributable under the GNU license. The most important (and in some cases quite unique) features of the codes follow:

- Solution of the system of PDEs is carried out monolithically, which means that the resultant numerical scheme is characterized by just one stiffness matrix. The PDEs are first rewritten into the weak forms whose numerical integration provides its coefficients. The integration is performed using the Gauss quadrature formulas.
- Fully automatic *hp*-adaptivity. In every iteration step the solution is compared with the reference solution (realized on an approximately twice finer mesh), and the distribution of error is then used for selection of candidates for adaptivity. Based on sophisticated and subtle algorithms the adaptivity is realized either by a subdivision of the candidate element or by its description by a polynomial of a higher order [14].
- Each physical field can be solved on quite a different mesh that best corresponds to its particulars. Special powerful higher-order techniques of mapping are then used to avoid any numerical errors in the process of assembly of the stiffness matrix.
- In nonstationary processes every mesh can change in time, in accordance with the real evolution of the corresponding physical quantities.
- Easy treatment of the hanging nodes [15] appearing on the boundaries of subdomains whose elements have to be refined. Usually, the hanging nodes bring about a considerable increase of the number of the degrees of freedom (DOFs). The code contains higher-order algorithms for respecting these nodes without any need of an additional refinement of the external parts neighboring with the refined subdomain.
- Curved elements able to replace curvilinear parts of any boundary by a system of circular or elliptic arcs. These elements mostly allow reaching highly accurate results near the curvilinear boundaries with very low numbers of the DOFs.

Agros2D also contains a module for the time integration of ordinary differential equations (describing motion of charged particles in an external electric field) based on an adaptive Runge–Kutta–Fehlberg algorithm (the time step is variable and depends on the actual development of the solution).

4. Shape optimization of electrodes

The optimization process was based on the minimization of two functionals F and G representing the accuracy of impact of PVC and PET particles,

respectively. Both functionals are calculated as an average distance of points, where particles impacted and desired positions on each side of the bottom of the separator model. In the case of multi-criteria optimization, more than one optimal design can be found. They are optimal in the sense that any improvement of one functional inevitably leads to worsening of the other functional. A set of such optimal solutions form the so-called Pareto front. The actual optimization has been carried out using one-criterion optimization by the conjugate-gradient method. We performed multiple optimizations using criteria function of the form

$$\alpha F + (1-\alpha) G \tag{7}$$

for different values $\alpha \in (0,1)$. This is a simple method to obtain the Pareto front.

The conjugate-gradient method is a very popular method for optimization calculations. It is a step method, based on the evaluation of gradients of steepest descend, that are in each step used to calculate direction, where a 1-dimensional optimization (so-called line search) is performed. In our calculations, we encountered problems with the gradient calculations. Although we tried to design our criteria functions to be smooth, we experienced problems calculating gradient components using standard formula. We had to use higher-order differentiation formula

$$f(x) = \frac{1}{12h}\left(-f(x+2h) + 8f(x+h) - 8f(x-h) + f(x-2h)\right), \tag{8}$$

so we could use large enough h to achieve correct results. Gradient values were not reliable for too small values of h.

5. Illustrative example

The described way of computation is applied to a separator of granular material. The material consists of polyvinyl chloride (PVC) and polyethylenterephthalat (PET) grinded to small spherical particles. The basic geometry of the separator is depicted in Fig. 2. The electrodes (prior to the optimization process) are planar.

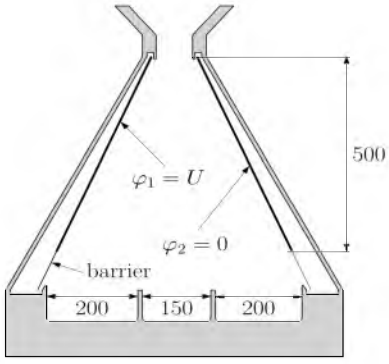

Fig. 2. Basic geometry of the separator (dimensions in mm)

The charges and dimensions of the particles under consideration obey the normal distribution with parameters listed in Tab. 1. Their numbers $n = 250$ for each kind of material. The voltage U between the electrodes is variable. The task is to map the trajectories of the particles, optimize the shape of the electrodes and find the efficiency of the device before and after this shape optimization.

Table 1. Selected parameters of the particles

Type	Density	Radius		Charge	
	ρ (kg/m^3)	μ (mm)	σ (mm)	μ (C)	σ (C)
PVC	1370	2	0.25	–0.5E–9	0.8E–10
PET	1330	2	0.25	+0.25E–9	0.8E–10

Symbol μ denotes median, symbol σ stands for variance

For example, figures 3, 4 and 5 show the distributions of the radii and charges of the PVC and PET particles.

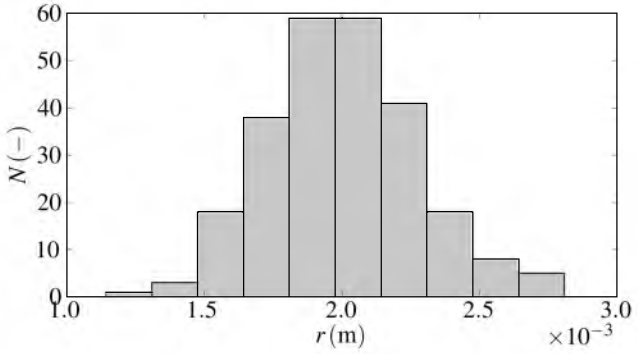

Fig. 3. Distribution of radii of the PET and PVC particles

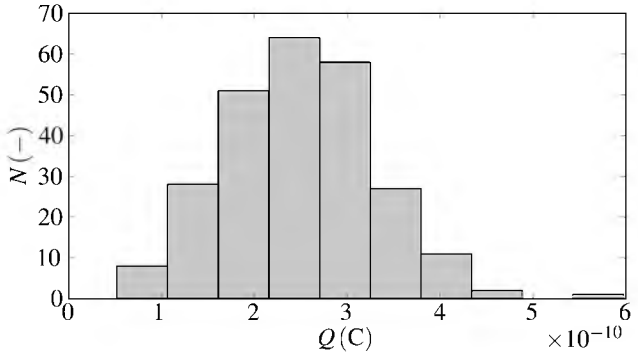

Fig. 4. Distribution of charges of the PET particles

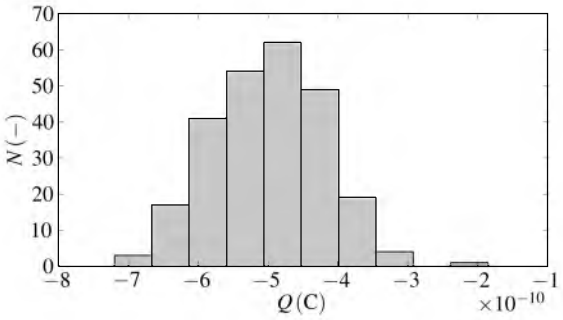

Fig. 5. Distribution of charges of the PVC particles

The computations of electric field in the system were carried out using the *hp*-adaptivity with prescribed tolerance of 3 %. The process of adaptivity required 6 iteration steps starting from the rough mesh with polynomial order $p = 1$. After finishing the adaptive process the maximum order of polynomials is 8 and the number of the degrees of freedom (DOFs) is 3624. The final mesh is shown in Fig. 6; the rectangles on the right side contain the orders of polynomials in particular elements of the mesh. The convergence curve of the adaptive process is shown in Fig. 7. The black circles on it show the situation after particular iteration steps.

Figure 8 shows the distribution of the electric field in the system, after optimizing the shape of the electrodes. Its module varies almost linearly with height within the range from 200 kV/m (feeder) and 45 kV/m (recycle bins).

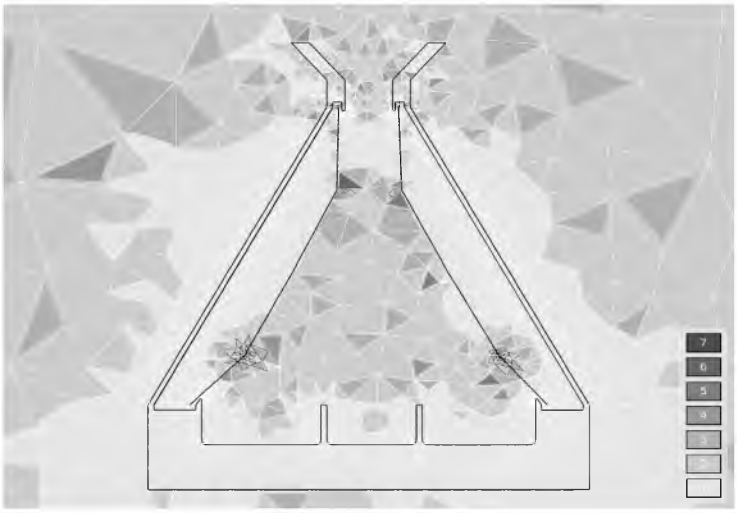

Fig. 6. Final mesh after the adaptive process (relative error 2.426 %, 3264 DOFs, 6 steps)

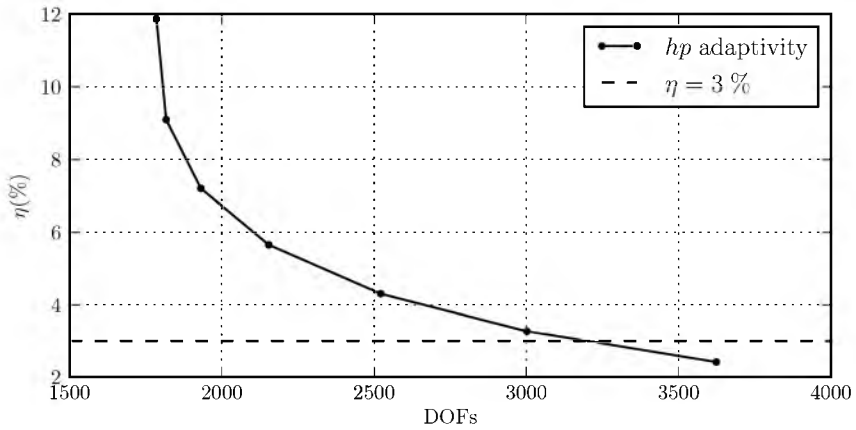

Fig. 7. Dependence of relative error on number of DOF during the adaptive process

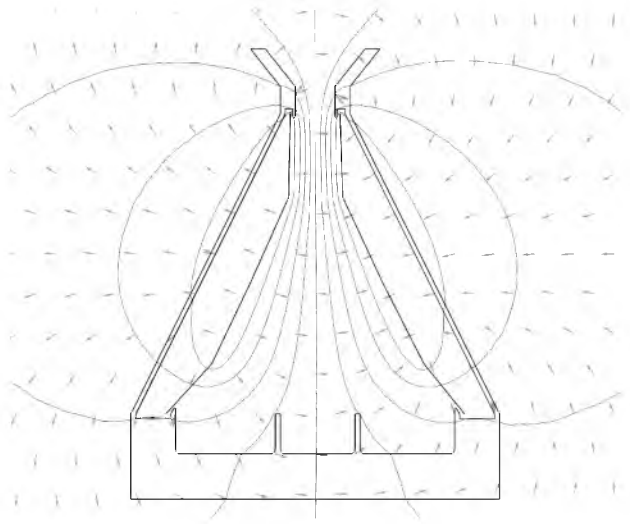

Fig. 8. Equipotential lines and vectors of the electric field in the system

For this optimized arrangement we determined the trajectories of both types of particles and found the dependence of efficiency of the device on the voltage between the electrodes (which will be shown later). Then we started optimizing the electrodes.

Figure 9 shows the corresponding Pareto front discussed in section 4. This front was obtained in two ways: using the conjugate gradients and random selection. Evaluation of this front lead to new shapes of electrodes (see Fig. 10) whose electric field makes more charged particles fall down to the correct bins.

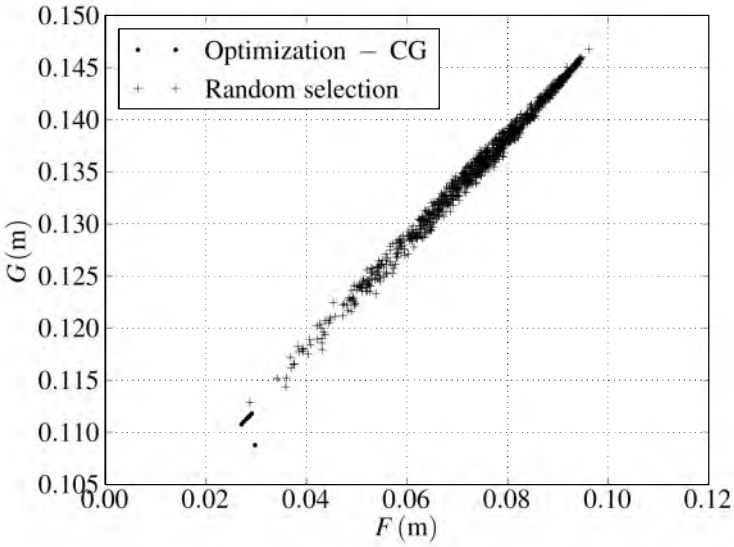

Fig. 9. The Pareto front for the optimization problem

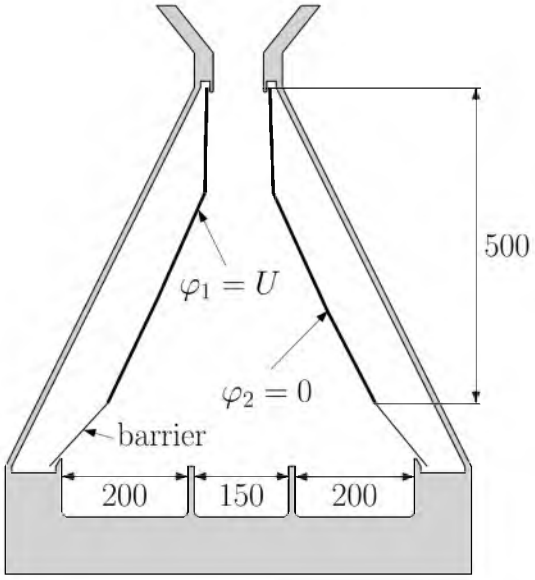

Fig. 10. Optimized arrangement of the electrodes

Figure 11 shows, for illustration, selected trajectories of the PVC (left) and PET (right) particles in the electric field generated by the optimized electrodes.

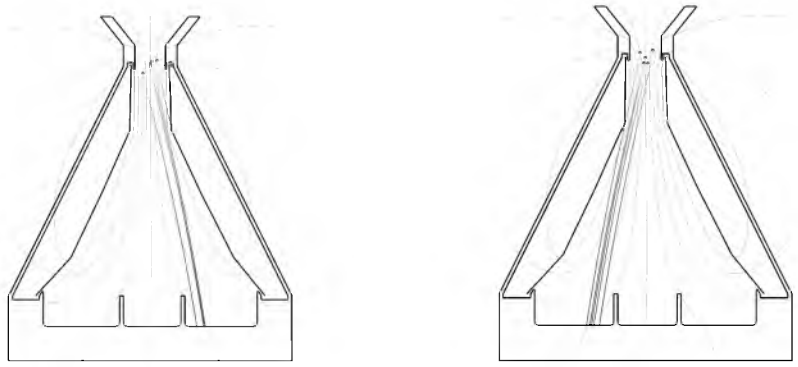

Fig. 11. Trajectories of the PVC (left) and PET (right) particles in the optimized arrangement

The efficiency of the separation process expressing how many particles fall down to the appropriate bins strongly depends on the voltage U. Its curves for both the basic and optimized arrangements are depicted in Fig. 12. The efficiency of the optimized variant is higher by about 20 %.

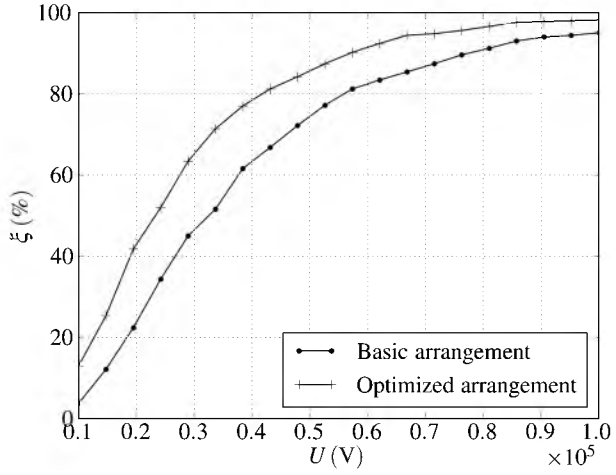

Fig. 12. Efficiency of the separation process as a function of voltage for the basic and optimized arrangements

6. Conclusion

The optimization of the system consisting of finding the most appropriate shape of the electrodes may lead to a considerable improvement of the efficiency of the device even more than by 20 %. In the next phase of the work, a physical model of the device will be built for experimental validation of the anticipated results.

Acknowledgment

This work was supported by the European Regional Development Fund and Ministry of Education, Youth and Sports of the Czech Republic (project No. CZ.1.05/2. 1.00/03.0094: Regional Innovation Centre for Electrical Engineering - RICE) and by the Grant project GACR P102/11/0498.

References

[1] Pearse M. J., Hicky T. J., The Separation of Mixed Plastics Using a Dry Triboelectric Technique, Resource Recovery and Conservation, Volume 3, No. 2, pp. 179–190, 1978.

[2] Yanar D. K, Kwetkus B. A., Electrostatic Separation of Polymer Powders, Journal of Electrostatics, Volume 36, No. 2–3, pp. 257–266, 1995.

[3] Higashyiama Y., Asano, K., Recent Progress in Electrostatic Separation Technology, Particulate Science and Technology, Volume 16, No. 1, pp. 77–90, 1998.

[4] Inculet I. I., Castle G. S. P., Brown J. D., Electrostatic Separation for Recycling, Particulate Science and Technology, Volume 16, No. 1, pp. 91–100, 1998.

[5] Dodbiba G., Shibayama A., Miyazaki T., Fujita T., Triboelectrostatic Separation of ABS, PS and PP Plastic Mixtures, Material Transactions, Volume 44, No. 1, pp. 161–166, 2003.

[6] Wei J., Realff M. J., Design and Optimization of Free-Fall Electrostatic Separators for Plastics Recycling, AIChE Journal, Volume 49, No. 12, pp. 3138–3149, 2003.

[7] Saeki M., Triboelectric Separation of Three-Component Plastic Mixture, Particulate Science and Technology, Volume 26, No. 5, pp. 494–506, 2008.

[8] Tilmatine A., Medles K., Younes M., Bendaoud A., Dascalescu L., Roll-Type versus Free-Fall Electrostatic Separation of Tribocharged Plastic Particles. IEEE Trans. Industry Appl., Volume 46, No. 4, pp. 1564–1569, 2010.

[9] Moesner F. M., Toshiro H., Contactless Manipulation of Microparts by Electric Field Traps. Proc. SPIE's Int. Symposium on Microrobotics and Microsystem Fabrication, October 1997, Pittsburgh, USA, Volume 3202, pp. 168–175.

[10] Duff N., Lacks D. J., Particle Dynamics Simulation of the Effect of Particle Size Distribution on Triboelectric Charging in Granular Insulator System, Journal of Physics, Conference Series, Volume 142, No. 1, 2008, doi:10.1088/1742-6596/142/1/012078.

[11] Kuczmann M., Iványi A., The Finite Element Method in Magnetics, Akademiai Kiadó, Budapest, 2008.

[12] Code Agros2D: http://agros2d.org.

[13] Code Hermes2D: http://hpfem.org/hermes.

[14] Šolín P., Segeth K., Doležel I., Higher-Order Finite Element Methods, Chapman & Hall/CRC, Boca Raton, FL, USA, 2003.

[15] Šolín P., Červený J., Doležel I., Arbitrary-Level Hanging Nodes and Automatic Adaptivity in the *hp*-FEM, Math. Comput. Simul., Volume 77, No. 1, pp. 117–132, 2008.